Journal of Applied Polymer Science

Poly(vinyl alcohol) modified by KE reactive dyes as a novel proton-exchange membrane for potential fuel-cell applications

Tianchi Zhou,[1,2] Xuemei He,[2] Kongliang Xie[1]

[1]College of Chemistry, Chemical Engineering, and Biotechnology, Donghua University, 2999 Ren'min North Road, Shanghai 201620, China

[2]YanCheng Institute of Technology, 9 Ying'bing Road, Yancheng 224051, China

Correspondence to: K. Xie (E-mail: 120413181@qq.com)

ABSTRACT: A new type of proton-exchange membrane based on poly(vinyl alcohol) (PVA) modified KE reactive dyes (KE-4BD) was prepared and evaluated as H^+-conducting polymer electrolytes. The effects of the content of KE-4BD on the membrane H^+ conductivity and water uptake were studied with an alternating-current impedance technique and the method of weighing, respectively. Fourier transform infrared and scanning electron microscopy were used for the chemical and structural characterization of these membranes. With all of these properties, the optimal mass ratio between PVA and KE-4BD was 1:0.5, and the resulting membrane exhibited a high proton conductivity (0.109 S/cm) at room temperature; this afforded a power density of 83.9 mW/cm^2 at 210.4 mA/cm^2 and an open-circuit voltage of 810.8 mV. The PVA/KE-4BD membranes showed a high oxidative stability in Fenton's reagent (3% H_2O_2 v/v, 2 ppm $FeSO_4$). Thermal analysis also showed that the membranes exhibited a significant improvement in thermal stability. © 2015 Wiley Periodicals, Inc. J. Appl. Polym. Sci. **2016**, *133*, 43019.

KEYWORDS: dyes/pigments; electrochemistry; membranes

Received 13 April 2015; accepted 5 October 2015

DOI: 10.1002/app.43019

INTRODUCTION

In recent years, a high energy demand and an urgent need for environmental protection have become two of the most important topics in the sustainable development of mankind. Efforts to reduce dependency on fossil fuels and to explore environmentally friendly, clean, and sustainable energy sources have become more extensive in the last 2 decades. Fuel cells, particularly polymer electrolyte membrane fuel cells using proton-exchange membranes (PEMs), have been considered one of the most promising technologies because of their high energy efficiency, high energy/power densities, low/zero emissions, and wide application areas in portable, stationary, and automobile powers.[1,2] Among the membranes used in fuel cells, Nafion membranes have been most widely used because of their high chemical, electrochemical, and mechanical stabilities and high proton conductivity (ca. 10^{-1} S/cm) at ambient temperature.[3] However, some challenges still hinder their real commercialization, for example, their high cost, which is due to their complex synthesis and processing; high methanol permeability; potential health and environmental issues; and instable proton conductivity.[4,5]

Recently, great interest has been shown in the search for new nonfluorinated membrane materials with low cost and their required electrochemical characteristics. Novel PEMs, such as polymeric membranes, ceramic membranes, and inorganic–organic membranes, have been greatly developed.[6] In all of these novel membranes, the development of hydrocarbon polymeric PEMs has increasingly become a very important research direction. Generally, this type of PEM is built from two parts: the polymer, which acts as a matrix, and many proton-conductive functional groups, such as sulfonic acid[7,8] or phosphonic acid,[9] which are introduced to the main chain or side chains of the polymer to transfer protons from one group to another. Many polymers, including poly(*p*-phenylene),[7,10] poly(arylene ether ketone),[8,11] polysulfone,[12] poly(arylene ether sulfone),[13–15] poly(aryl ether ether nitrile),[16,17] poly(sulfide ketone),[18] polyimide,[19,20] poly(2,6-dimethyl-1,4-phenylene oxide),[21] and polybenzimidazole,[22–24] have been applied the preparation of membranes. The basic requirements of a PEM for use in fuel cells are that it should have good mechanical properties, thermal stability, a high performance–price ratio, and a high H^+ conductivity. However, these membranes have shortcomings, including a high price,[22–24] difficulty in the synthesis process,[11] and easy solubility in hot water.[8,13] Therefore, rational molecular and membrane design is still a big challenge for PEMs in fuel-cell technology.

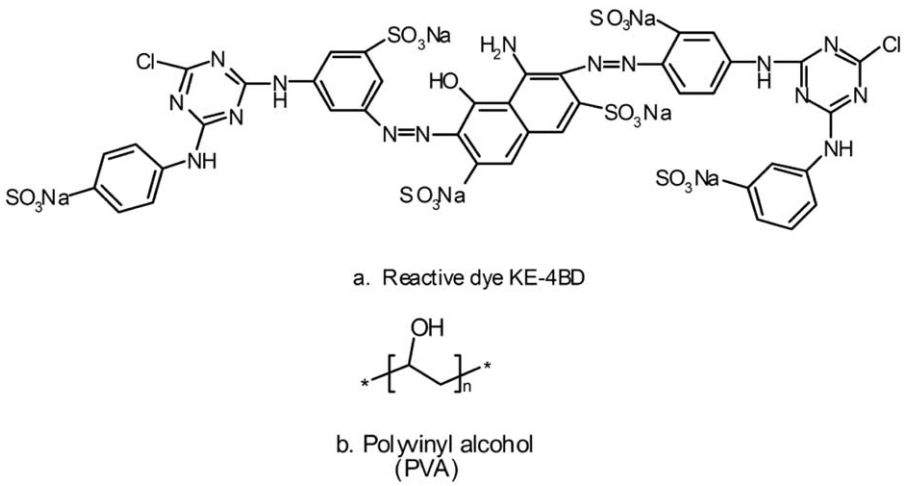

Figure 1. Chemical structures of the (a) reactive dye KE-4BD and (b) PVA.

Poly(vinyl alcohol) (PVA)-based membranes are one of the main research objects because of the following advantages: easy preparation, biodegradability, chemical stability, hydrophilic properties, low cost, reduced ethanol permeability, good mechanical properties, reactive chemical functions favorable for crosslinking or grafting, and excellent film-forming properties.[25–28] However, pristine PVA does not have the ability to conduct H^+ for the absence of specific functional groups; hence, it must be used in conjunction with other materials by means of blending, chemical modification, doping with inorganic fillers, or forming hybrid structures.[29–34] Thanganathan and Nogami[33] prepared PVA-based hybrid membranes incorporating inorganic fillers and ionic liquids. The thermal stability of both membranes was present up to 370°C, but the ionic conductivity was only 0.83×10^{-3} and 0.58×10^{-3} S/cm, respectively, at 60°C. Qiao *et al.*[32] reported a series of proton-conducting membranes based on chemically crosslinked PVA–poly(2-acrylamido-2-methyl-1-propanesulfonic acid) (PAMPS); these showed high proton conductivities up to 0.06–0.1 S/cm, where PAMPS was successfully retained in the membrane by the formation of a semi-interpenetrating polymer network. However, PAMPS is a water-soluble polymer and can be gradually lost during the period of use. Gomes and Filho[34] constructed hybrid PVA-based membranes with phosphotungstic acid to dope into the PVA matrix; this provided proton conductivity, and PVA was crosslinked by (diethylenetriamine)pentaacetic acid, but the proton conductivity of the membrane was also on the order of 10^{-3} S/cm.

Polyfunctional reactive dyes were developed for cotton dyeing in the early 1950s. These dyes contained more than two reactive sites to form covalent bonds with nucleophilic sites in the substrates and also contained several sulfonic groups to provide water-soluble properties. In this study, a novel PEM system was designed, in which PVA [Figure 1(b)] was selected as the host polymer and a bifunctional reactive dye, KE-4BD [Figure 1(a)], containing sulfonic groups, was chosen to provide charge-carrier-conducting protons. By the way of blending and dyeing, KE-4BD was firmly fixed on the PVA matrix by the substitution reaction of nucleophilic SN2 as described:

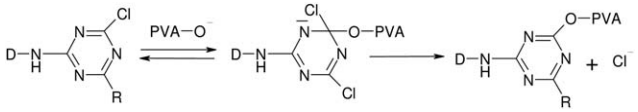

Furthermore, compared to polymers that get sulfonic groups via sulfonation in sulfuric acid (which may cause side reactions that result in a decrease in the proton conductivity)[35,36] or radiation grafting methods (which may lead to considerable deterioration in the mechanical properties),[37,38] the original performance of the matrix with this method was less affected because of the moderate chemical modifications.

The membranes prepared in this study were examined with Fourier transform infrared (FTIR) spectroscopy and scanning electron microscopy (SEM) to analyze their chemical structure and morphological microstructure. Thermogravimetric analysis was adopted to study the thermal stability. The membrane characteristics, including the H^+ conductivity, water uptake, and oxidative stability, were studied to evaluate their application performances. Finally, these membranes were used to fabricate membrane electrode assemblies (MEAs) for actual H_2/O_2 single fuel cells.

EXPERIMENTAL

Materials and Membrane Preparation

A stock 6% PVA (99% hydrolyzed, weight-average molecular weight = 86,000–89,000, Aldrich) aqueous solution was prepared by the dissolution of PVA in distilled water at 80°C. The reactive dye KE-4BD (Wujiang Taoyuan Dyestuff Co., Ltd., China) was purified by a dimethylformamide–acetone method before it was separately made into solutions with different concentrations and then mixed with the previous PVA solution under stirring for at least 60 min to ensure that the new solution was completely homogeneous. After completed mixing, the solution was heated to 80°C and stirred at this temperature for 2 h in a water

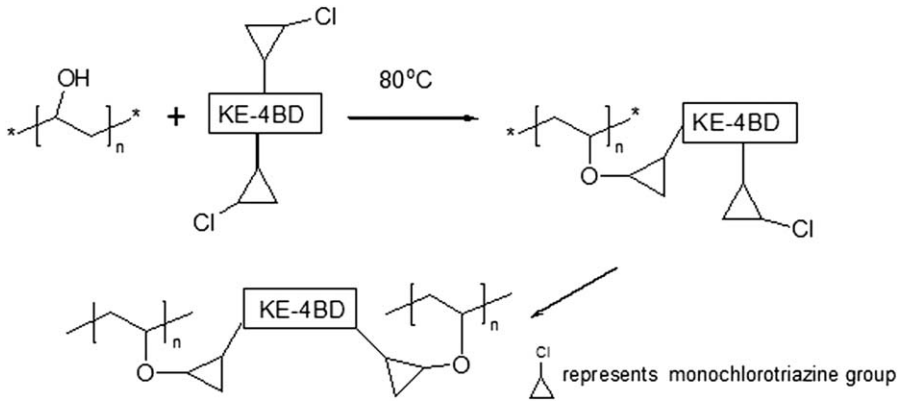

Figure 2. Reaction equation of the PVA by modified KE-4BD.

bath so that the chemical reaction, as shown in Figure 2, could be fully carried out. Then, the solution was degassed in a vacuum chamber, poured into plastic dishes, and dried under ambient conditions. Then, the membrane (Figure 3) was peeled away from the plastic dish and subsequently washed with soaping water (5 g/L soap flakes at room temperature); it was then thoroughly rinsed in tap water to remove unstable color before it was dried naturally.

To further reduce membrane swelling and improve the mechanical stability, we modified the membrane by crosslinking the PVA main chain with glutaraldehyde (GA) in the presence of a strong acid, as proposed by Qiao and coworkers.[39–42] Square samples of the membranes (ca. 1.5 × 1 cm^2) were soaked in a reaction solution consisting of 10 wt % GA and a small amount of HCl in acetone at 30°C for 30 min for chemical crosslinking.[39–42] Crosslinking proceeded between the —OH of PVA and the —CHO of GA in the polymer because of an acid-catalyzed reaction. Then, the membrane was soaked in 10 mL of a 1.0*M* HCl solution to convert the SO_3Na form into the SO_3H form. Before use, the membrane was washed with deionized water several times to remove excess HCl and was finally stored in a plastic sealed bag for measurements. Flat membranes were obtained with a thickness of about several tens of micrometers (50–70 μm), as measured by a micrometer. The inner chemical structure of the PVA/KE-4BD system is illustrated in Figure 4.

Figure 3. Picture of the PVA/KE-4BD PEM prepared by solution-casting technology with a plastic Petri dish as a container. [Color figure can be viewed in the online issue, which is available at wileyonlinelibrary.com.]

Characterization of the PVA/KE-4BD Membranes

FTIR spectra were recorded on an FTIR-4200 spectrometer (Shimadzu, Japan) equipped with attenuated total reflectance instrument, which was used to obtain the spectrogram in the range from 4000 to 600 cm^{-1}. Air was used as a background reference.

A Quanta 200 SEM analyzer (FEI) was used to observe the cross-profile morphology of the membranes. Before observations, the membrane samples were sputtered with gold and then examined at 10,000× magnification.

Thermogravimetric analysis of the membrane was performed with an STA449C apparatus (Netzsch, Germany). Samples of about 10 mg were loaded into an aluminum pan and then heated from 30 to 650°C at a rate of 10°C/min under an air atmosphere. The vacant aluminum pan was used as a reference throughout the whole experiment.

Ion-Exchange Capacity (IEC)

The IEC (mequiv/g of the PVA/KE-4BD membranes) was determined by a titration method. Square pieces of the membranes were set in 20 mL of a 1*M* NaCl solution at room temperature for 24 h to replace the protons with sodium ions. The H^+ ions released from the membranes were then titrated to the end point with a 0.1*M* NaOH solution with phenolphthalein as the indicator. The IEC (mequiv/g) was calculated as the ratio of exchangeable protons to the weight of dried sample via the following formula:

$$\mathrm{IEC} = V_{\mathrm{NaOH}} C_{\mathrm{NaOH}} / W_{\mathrm{dry}}$$

where V_{NaOH} is the consumed volume of NaOH, C_{NaOH} is the molar concentration of NaOH, and W_{dry} is the weight of the dried membrane.

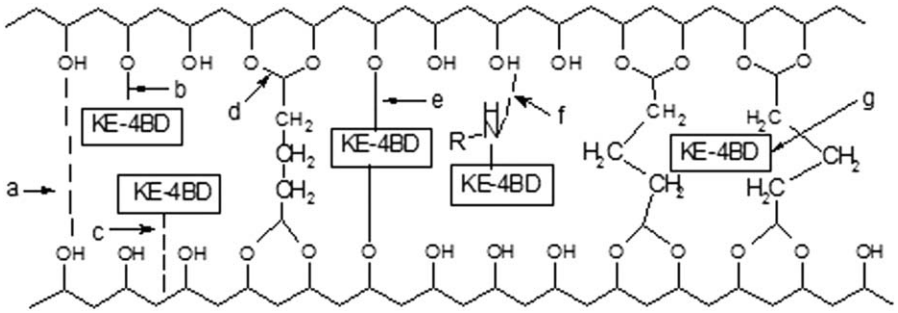

Figure 4. Inner structure of a chemically crosslinked PVA/KE-4BD PEM: (a) hydrogen bonds, (b) grafting, (c) van der Waals forces, (d) aldol condensation, (e) crosslinking, (f) hydrogen bonds, and (g) doping.

Water Uptake

The swelling of the membranes was evaluated by the water uptake of the membranes (g/g), which was estimated from the mass change before and after the complete drying of the membrane. The dry membrane was swollen in deionized water at 20°C for a day, then the surface water was wiped carefully with a filter paper, and the membrane was weighed immediately. After the sample was dried overnight in a vacuum oven at 60°C, the water uptake was calculated with the following expression:

$$\text{Water uptake} = \left(W_{\text{wet}} - W_{\text{dry}}\right)/W_{\text{dry}} \quad (1)$$

where W_{wet} is the mass of the fully hydrated membrane.

Proton Conductivity

The proton (H^+) conductivity of the formed membrane was measured by an alternating-current impedance technique with a Zahner Zennium electrochemical impedance analyzer, where the alternating-current frequency was scanned from 1 MHz to 0.1 Hz at a voltage amplitude of 50 mV. Fully hydrated membranes were sandwiched in a Teflon conductivity cell equipped with Pt foil contacts on which Pt black was plated (Figure 5). The membrane was in contact with water throughout the measurement. The impedance was measured at room temperature. The ionic conductivity (σ; S/cm) was calculated according to the following equation:

$$\sigma = l/(RA) \quad (2)$$

where l and A are the thickness and contact area of the membrane sample, respectively, and R is the membrane resistance.

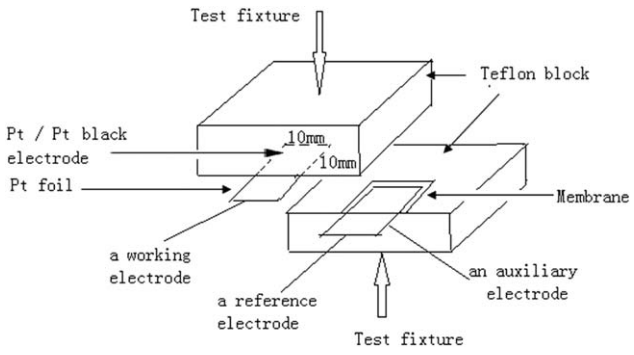

Figure 5. Schematic diagram for ionic conductivity measurement.

Membrane Stability

The oxidative stability of PVA/KE-4BD was tested by a Fenton reagent in an aqueous solution of H_2O_2 (3%)/$FeSO_4$ (2 ppm) and was tracked by the measurement of the weight loss as a function of the immersion time at a fixed treatment temperature of 60°C.

Single-Cell Performance Measurement

The catalyst slurry was prepared by the mixture of 40%Pt/C (E-TEK) with a 5 wt % Nafion solution (DuPont) for the ink. For fabrication of the MEA, the catalyst slurry was coated on carbon paper (Toray TGP-H-090) to give a metal loading of 2 mg/cm^2 on the anode. The catalyst loading on the cathode was 1 mg (Pt)/cm^2. The binder loadings on both electrodes were 0.6–1.0 mg/cm^2. MEA was prepared by the hot pressing of the anode and cathode to the prepared membrane at a pressure of 100 kg/cm^2 at 110°C for 5 min. The active area for a single-cell test was 4 cm^2.

The MEA was inserted into single-fuel-cell hardware, which consisted of a graphite block with an active electrode area of 4 cm^2, a machined serpentine flow channel, and golden current collectors. Pure hydrogen and oxygen were supplied to enter the anode and cathode channels under atmospheric pressure at flow rates of 100 and 70 mL/min, respectively, through a humidifier maintained at 25°C under ambient pressure. Polarization curves were obtained with a fuel-cell evaluation system (GE/FC1-100).

RESULTS AND DISCUSSION

FTIR Studies

The IR spectra of the pristine PVA and PVA/KE-4BD membranes (1:0.5 mass ratio) are shown in Figure 6. It was clear that the absorption peaks between 3300 and 3400 cm^{-1} in both spectra were due to the stretching vibrations of the —OH groups from PVA and the —NH— groups from KE-4BD. The bands between 2840 and 2950 cm^{-1} arose from the stretching of saturated C—H groups. The peak at 1716 cm^{-1} in the curve of PVA/KE-4BD was due to the stretching of carbonyl groups from crosslinked PVA/KE-4BD because of the free —CHO of GA.[39–42] The appearance of the peaks centered at 1639 and 1432 cm^{-1} corresponded to the vibrations of C=N and C=C of KE-4BD; they indicated that KE-4BD was successfully incorporated into the polymer matrix. The appearance of the sulfonate stretching peak at 1044 cm^{-1} also clearly demonstrated the effective incorporation of the dye into the PVA membranes. The

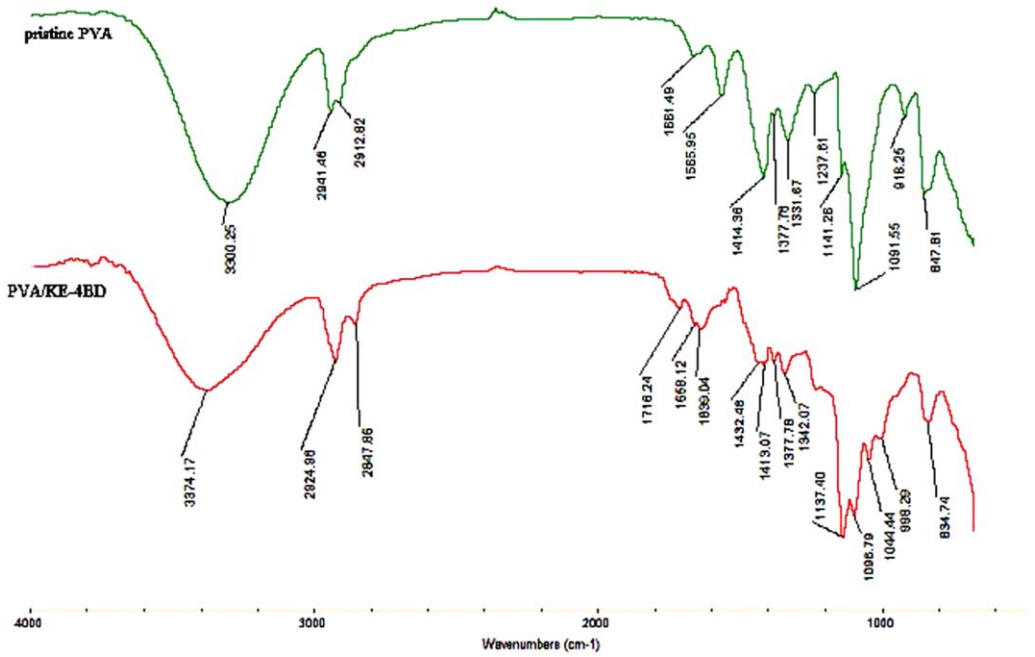

Figure 6. FTIR spectra of the pristine PVA and PVA/KE-4BD membrane. [Color figure can be viewed in the online issue, which is available at wileyonlinelibrary.com.]

peak at 1137 cm^{-1} might have arisen from C—O—C groups, and the peak at 998 cm^{-1} might have been related to =C—O—C in the PVA/KE-4BD membrane. These two peaks might have been caused by the S_N2 reaction between the —OH of PVA and the bichloro-*s*-triazine groups of KE-4BD. The previous results show that because of the successful incorporation of KE-4BD in the PVA matrix, the as-prepared membrane provided good H^+ conductivity, as discussed later.

SEM Images of the PVA/KE-4BD Membranes

Figure 7 shows the cross-sectional SEM pictures of the PVA/KE-4BD PEMs with different mass ratios. The dye molecules could be adopted into the PVA polymer matrix because of the various forms of bonding forces. We observed clearly that for PVA/KE-4BD at a low mass ratio of 1:0.25, the membrane was homogeneous without the formation of any microvoids, which are typically observed in many polymer films.[43,44] Obviously, this was attributed to the uniform distribution of KE-4BD dyes, which had adequate reactions with PVA and GA. However, the cross-profile became rough with increasing KE-4BD content in the polymer, particular in PVA/KE-4BD with a mass ratio of 1:0.5. The high KE-4BD content meant a high content of activate sulfonate groups in the neutral polymer matrix; this could improve the electric conduction function but, at the same time, resulted in aggregation in the membranes because of more unreacted dyes and more residual impurities, which were not removed completely in the purification step. In addition, the microstructure of the membrane changed after the dyeing and crosslinking process. On the basis of previous observations, the uniform and density network structure could not be formed, and the structure of the membrane (1:0.5 mass ratio) became relatively loose, and this was beneficial for improving the membrane's conductivity.

Thermal Analysis

Figure 8 shows the thermogravimetric profiles of the PVA/KE-4BD acid PEMs at different contents of KE-4BD in the polymer under air conditions. Thermal analysis in most studies is always

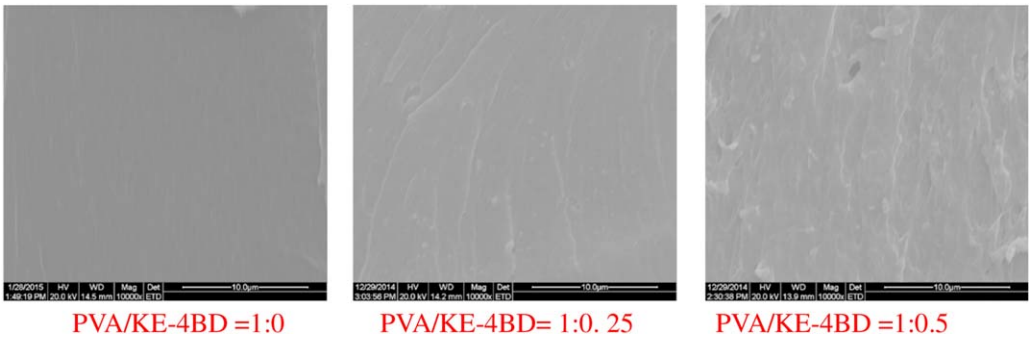

Figure 7. Cross-profile SEM pictures of the PVA/KE-4BD acid PEMs. [Color figure can be viewed in the online issue, which is available at wileyonlinelibrary.com.]

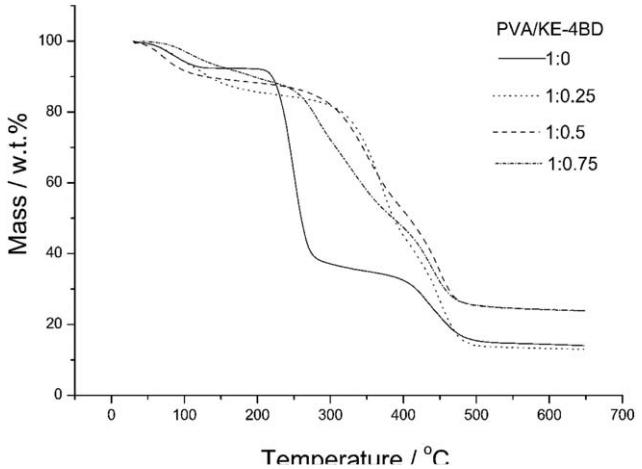

Figure 8. Thermogravimetric analysis profiles of the PVA/KE-4BD acid PEMs.

performed under nitrogen,[45–47] but in this study, air was adopted as the atmosphere to carry out the measurement because the membrane contacted oxygen during the working process. All of the samples displayed three major weight loss stages around 80–200, 220–380, and 400–480°C. The initial weight loss of the membranes (80–200°C) mainly belonged to the expulsion of water molecules or the moisture absorbed from the air from the polymer matrix. The second region (220–380°C) was the main thermal degradation process of the membranes, including the oxidative cleavage of the C—C backbone of the PVA main chain, the destruction of the crosslinking bridge, the decomposition of the reactive dye KE-4BD, and its partial separation from the PVA main chain. The third region (400–480°C) was attributed to the further oxidative decomposition and the char oxidation processes.[48–51]

As shown in Figure 8, the pristine PVA remained stable up to 210°C. After modification by KE-4BD and GA, the membranes were thermally stable up to 320°C, and we observed that an increased content of KE-4BD in the polymer led to an increase in the thermal onset degradation temperature. This could be explained by the fact that the crosslinking and strong hydrogen bonding were formed among PVA, GA, and KE-4BD; this provided the membrane with a high thermal stability. The PVA/KE-4BD membranes showed a much higher thermal onset degradation temperature above 210°C; this indicated a sufficient thermal stability for general fuel-cell operation temperatures under 100°C. This effect was confirmed in the second region (220–380°C), where the weight loss curve for the pristine PVA dropped dramatically, whereas the decomposition of the modified membranes was slower. This indicated that the heat release was markedly reduced. Furthermore, the temperatures of 50% weight loss (TG-50%) were 380°C (PVA/KE-4BD = 1:0.25), 385°C (PVA/KE-4BD = 1:0.5), and 408°C (PVA/KE-4BD = 1:0.75); they were all higher than the 260°C of pristine PVA. The percentage of remaining residues of the modified membranes were about 23.85% (PVA/KE-4BD = 1:0.5) and 23.90% (PVA/KE-4BD = 1:0.75) compared to 14.02% for the pristine PVA membrane at 650°C. All of these data indicate that the thermal stability of these modified membranes showed good improvement.

IEC, Water Uptake, and Ionic Conductivity

As an indicator of a polymer membrane's capacity to exchange ions, the IEC is closely related to the proton conductivity and, thus, has a major effect on membrane performance. From the data in Table I, one can see the IEC values of the prepared PVA/KE-4BD membranes from the titration test were in the range 0.44–1.61 mequiv/g. With mass ratios from 1:0.125 to 1:1, the IEC values increased with increasing KE-4BD content. The increased IEC values could be explained by the following two facts. One was that because of the increased sulfonic groups with increasing content of KE-4BD in the membrane, the charge carriers were increased because the number of exchangeable H^+ increased. The other reason may have been the fact that the structure of the membrane became relatively loose with increasing content of KE-4BD in the membrane. This may have provided more H^+ groups entering into the internal structure of the membrane during the ion-exchange process.

As we all know, proton transport and diffusion in the membrane always obey two mechanisms: the Grotthuss model and the vehicle mechanism. Possibly, the former is performed by bound water, and the latter is done by free water,[52] so water uptake is one of the essential features of membranes. Generally speaking, the ionic conductivity will increase with increasing water uptake because water clusters can offer transport channels for H^+ inside the membrane. However, if the membrane is too hydrophilic, excess water inside the membrane can dilute the charge carrier and has negative effects on the H^+ conductivity.[53] Furthermore, an excessively high water uptake can increase the membrane's fragility; this makes it less durable when used in fuel cells. To obtain long-term stability, a membrane's water uptake should be optimized with respect to the ionic conductivity and flexibility performance. Chemical crosslinking is an effective means of limiting the swelling; this is of great importance for proton-conducting polymer membranes.

Figure 9 shows the Nyquist plot of the PVA/KE-4BD membranes with different mass ratios. Table I shows the typical effects of different contents of KE-4BD on both the water uptake and H^+ conductivity of the PVA/KE-4BD membranes. The related data of Nafion 212 are also listed in the table for comparison. We found that the ionic conductivity of the

Table I. Proton Conductivity, IEC, Water Uptake, and Membrane Flexibility of the PVA/KE-4BD and Nafion 212 Membranes

PVA/KE-4BD (mass ratio)	Water uptake (g/g)	IEC (mequiv/g)	σ (S/cm)	Membrane flexibility
1:0.125	0.92	0.44	0.028	○
1:0.25	1.29	0.81	0.074	○
1:0.50	1.76	1.35	0.109	○
1:0.75	2.05	1.52	0.127	△
1:1	2.54	1.61	0.123	×
Nafion 212	0.34	0.92	0.0972	○

○, flexible and tough; △, little e, brittle, and phase-separated; ×, very brittle and partially dissolved in water.

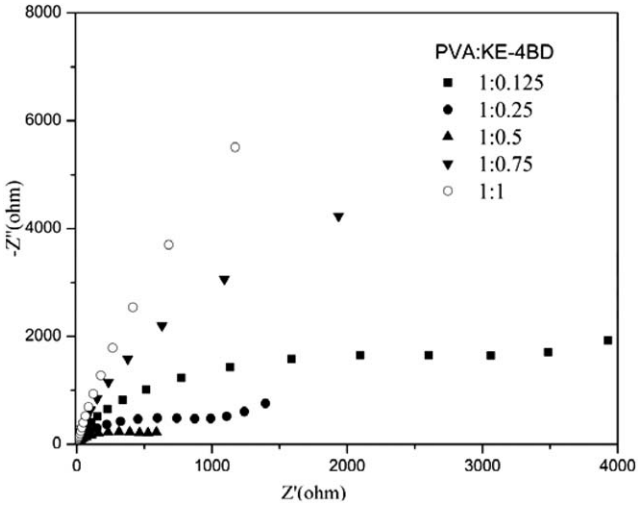

Figure 9. Nyquist plot of the PVA/KE-4BD membranes with different mass ratios. Z' and Z" are the real part and the imaginary part of impedance, respectively.

membranes strongly depended on the KE-4BD content and that the conductivity of the PVA/KE-4BD membranes with high KE-4BD content surpassed that of Nafion 212. The proton conductivity increased from 0.028 S/cm for PVA/KE-4BD with a mass ratio of 1:0.125 to 0.127 S/cm for PVA/KE-4BD with a mass ratio of 1:0.75. Such a conductivity increase was attributed to two factors: the high sulfonate content in the KE-4BD could have contributed to the proton conduction of the membranes, and the high water uptake, due to the presence of sulfonic acid groups with the water uptake being in excess of 2 g/g, could have contributed to the mobility of the ions. The proton conductivity initially increased quickly at first with increasing KE-4BD content and then slowed down. This could be explained by the fact that a further increase in the amount of water did not simply make an additional contribution to the conductivity but also led to a dilution of the charge carriers. Furthermore, too much KE-4BD could not be retained in the membrane because of the limited active points, and a high water uptake led to the extreme swelling of the membranes; this caused losses in the mechanical properties and dimensional stability. Moreover, excessive dyes may have gone out of the membrane with the flow of water, accumulated in the membrane's surface during the evaporation process, and could not contribute to the membrane's conductivity. Therefore, a PVA/KE-4BD mass ratio of 1:0.5 was seemingly optimal for practical fuel-cell usage. The proton conductivity of the PVA/KE-4BD membranes was comparable to those of some membranes, such as Nafion 212 membranes (0.0972S/cm at room temperature in our measurement), sulfonated poly(*p*-phenylene) derivative membranes (0.06–0.11S/cm at 30°C),[7] sulfonated naphthalene dianhydride based polyimide copolymer membranes (close to 0.1S/cm at 30°C),[54] side-chain poly(arylene ether ketone) functionalized with 1,4-butanesultone (SQNPAEK-*x*, "*x*" refers to the number of the attaching sulfobutyl groups in one unit) membranes (0.077–0.151 S/cm at 25°C),[11] sulfonated poly(arylene ether sulfone)s (0.02–0.1 S/cm at 30°C),[15] and PVA/PAMPS (0.075–0.16 S/cm at 25°C),[32] and was higher than those of some other membranes, such as pendant-sulfonated poly(arylene ether ketone) (PSPAEK)/organosiloxane polymer network (OSPN) semi-interpenetrating polymer network membranes (0.025–0.037S/cm at 40°C),[8] sulfonated copolyimide membranes (0.01–0.07 S/cm at 30°C),[20] PVA/SiO_2 hybrid membranes containing sulfonic acid groups (10^{-3} to 10^{-2} S/cm at 25°C),[30] sulfonated poly(ether ether ketone) membranes (0.0168S/cm at 80°C),[55] and polystyrene sulfonic acid (PSSA)/polyvinylidene fluoride (PVDF)/polyvinylpyrrolidone (PVP) membranes ($\sim10^{-2}$ S/cm at room temperature),[45] but the water uptake of the PVA/KE-4BD membranes was relatively high and will need to be adjusted in the future.

It is worth mentioning that crosslinking can affect the membrane's degree of swelling and structural density; these, in turn, affect the mechanical properties, stability in fuel cells, and mobility of the ions in the membrane. Generally speaking, because of the increased tortuosity in the membrane and the decreased hydrophilic groups with increasing crosslinking density, the proton mobility will be impeded, and the proton conductivity will suffer a corresponding decrease. Figure 10 shows the effect of different crosslinking times on both the water uptake and H^+ conductivity of the PVA/KE-4BD membranes. The crosslinking density could be elucidated by water uptake, and the experimental results indicate that the crosslinking density was closely correlated with crosslinking time. From the data listed in Figure 10, we observed that the water uptake value declined dramatically within the first hour of the crosslinking reaction; this indicated that as the number of hydrophilic hydroxyl groups continued to fall, the crosslinking density continued to increase, and the membrane was more hydrophobic as the reaction progressed. With extended crosslinking times, the decline tended to become slow and approached a plateau; this showed that the crosslinking reaction was finished completely. In addition, as shown in Figure 10, with the increasing crosslinking time, the conductivity of the membrane also declined sharply and then tended to gradually level off. Thus, with the consideration of the performance of water uptake, conductivity, and flexibility, the optimal crosslinking time was 30 min.

From Figure 11, it is clear that the contact angle of the PVA/KE-4BD membrane (1:0.5 mass ratio) before crosslinking was much bigger than that of the PVA/KE-4BD membrane after

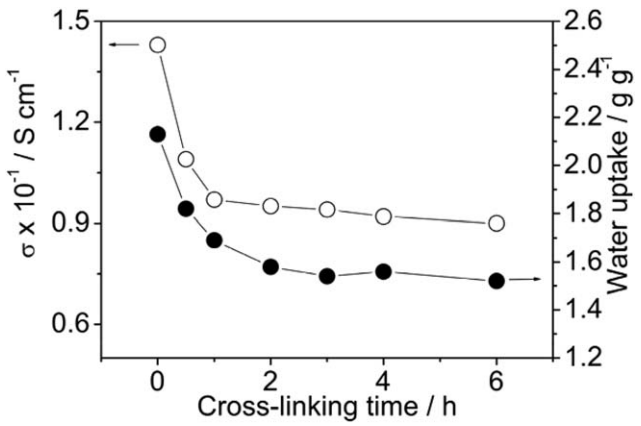

Figure 10. Effects of different crosslinking times on the proton conductivity and water uptake of the PVA/KE-4BD membranes.

Figure 11. Contact angles of the PVA/KE-4BD membrane before and after crosslinking.

crosslinking; this indicated further that the crosslinking step could effectively reduce the hydrophilic properties of the membranes.

Chemical Stability

The problem of a membrane's chemical stability is a big barrier that affects PEM fuel-cell performances. However, in many reports, the swelling behavior, proton conductivity, and MEA preparation have been the focus, but studies on oxidative stability have been relatively few.[34,35,56] To investigate whether the PVA/KE-4BD membranes had good antioxidant ability, the chemical stability of the PVA/KE-4BD membrane (1:0.5 mass ratio) was tested in Fenton reagent, that is, an aqueous solution of H_2O_2 (3%)/$FeSO_4$ (2 ppm), through the measurement of the weight loss as a function of the immersion time at a fixed treatment temperature of 60°C. As shown in Figure 12, the weight of the sample decreased slowly within the measuring period; this indicated that the membrane showed excellent oxidative longevity. An initial sharp decrease in the weight percentage (22.5%) was observed within 4 h, and then, the sample weight tended to remain about 70–75 wt % of the original up to 30 h, and the membrane still held about 70 wt % of its mass finally. The result shows that the performance of the PVA/KE-4BD membrane was significantly superior to those of hydrocarbon membranes with aromatic skeletons,[54,57,58] which were just subjected to treatment with deionized water at 80°C[50] or dissolved after being immersed in Fenton 's reagent at 80°C for 40–120 min.[11,57,58] Also, the membrane acquired very promising oxidation stability for application in fuel cell as a nonfluorinated hydrocarbon PEM.

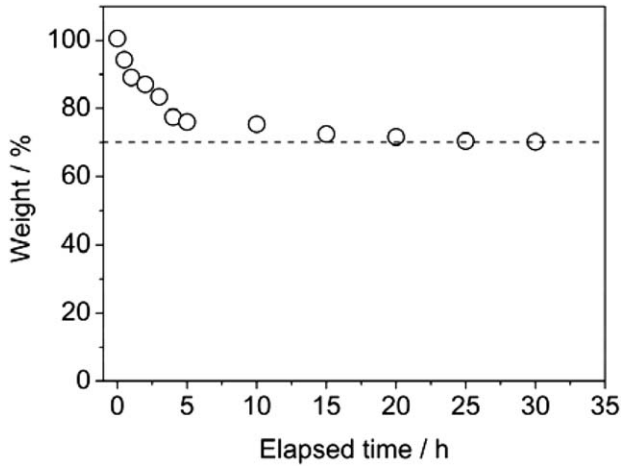

Figure 12. Time course of the PVA/KE-4BD membrane in H_2O_2 (3%)/$FeSO_4$ (2 ppm) at 60°C. The polymer mass ratio was 1:0.5 PVA/KE-4BD.

Single-Cell Performance

The MEA is one of the most important components impacting the overall performance of PEM fuel cells. Cell performances with PVA/KE-4BD (1:0.5 mass ratio)-fabricated MEA in H_2/O_2 mode were measured at room temperature. The anode stream was hydrogen with a flow rate of 100 mL/min, and the cathode stream was oxygen with a flow rate of 70 mL/min. As shown in Figure 13, the PVA/KE-4BD membrane showed that the open-circuit voltage was about 810.8 mV, and the peak power density was around 83.9 mW/cm^2 at 210.4 mA/cm^2. These values were comparable to those of the Nafion 212 membranes (95.1 mW/cm^{-2} at room temperature by our measurement). However, compared to some other membranes, such as membranes of sulfonated poly(arylene ether sulfone)s containing fluorophenyl pendant groups[15] (120.6 mW/cm^{-2} at 30°C) and chitosan/phosphotungstic acid polyelectrolyte membranes[59] (350 mW/cm^2 at 25°C), the PVA/KE-4BD membranes showed a lower cell performance. This was because, in addition to the PEM's properties, the cell behavior was also affected by the catalyst and the MEA fabrication procedures. The PVA/KE-4BD membrane may not

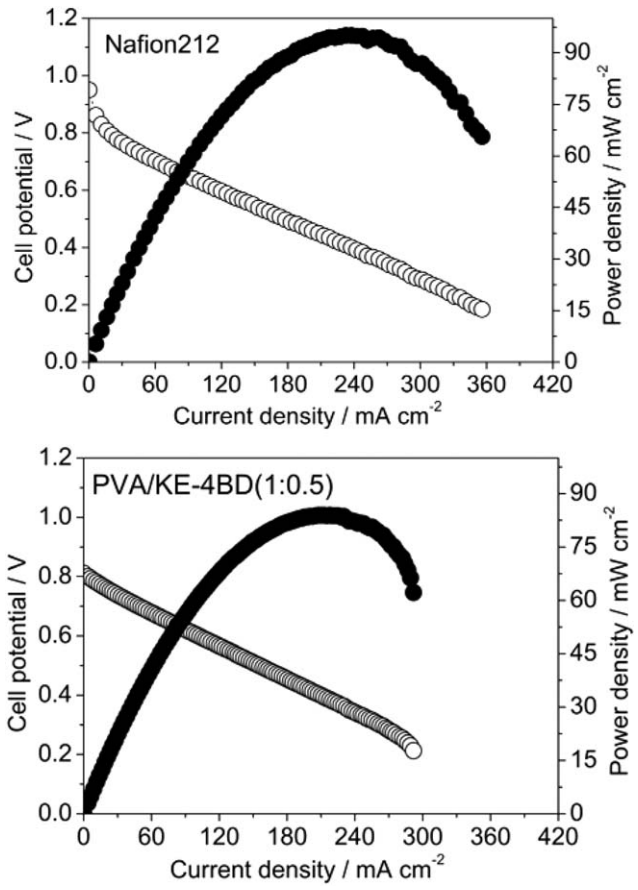

Figure 13. Polarization curves and power densities of the Nafion 212 and PVA/KE-4BD membranes (1:0.5 mass ratio) in the H_2/O_2 mode at room temperature.

have formed good contacts with both the catalyst and the gas-diffusion electrode; this, thereby, affected proton transfer between the membrane and Nafion-based catalyst layers. Further improvements in the performance of MEA testing are expected through optimization of new MEA fabrication techniques, new binders for the membranes, and the amount of catalyst loading.

CONCLUSIONS

In this study, novel PEMs from PVA/KE-4BD composites were prepared with combined blending and chemical crosslinking procedures. The resulting membranes exhibited high H^+ conductivities of 0.028, 0.074, 0.109, 0.127, and 0.123 S/cm at room temperature with increasing content of KE-4BD. After a consideration of all of the properties, the optimal mass ratio between PVA and KE-4BD was found to be 1:0.5, and the membrane showed a peak power density of 83.9 mW/cm^2 at 210.4 mA/cm^2 and open-circuit voltage of 810.8 mV at room temperature. Moreover, the membranes' chemical and micromorphology, as characterized by FTIR spectroscopy and SEM, proved that the membranes possessed the power to conduct H^+. Because of the compact and dense network structure among PVA, KE-4BD, and GA, the membranes showed excellent thermal stability. Meanwhile, the PVA/KE-4BD membranes also displayed a relatively high oxidative durability in an aqueous solution of H_2O_2 (3%)/$FeSO_4$ (2 ppm) at 60°C. All of the good properties suggested that the PVA/KE-4BD membranes could be new prospects for use in PEM fuel cells.

ACKNOWLEDGMENTS

This work was financially supported by the Industry–Academia–Research Joint Innovation Fund of Jiangsu Province (contract grant number BY2015057-06) and the Nature Science Foundation of Jiangsu Province (contract grant number BK20141261). Great thanks go to Donghua University, the Yancheng Institute of Technology, Jiangsu Zhongzhan Vehicle Accessories Co., Ltd., Wujiang Taoyuan Dyestuff Co., Ltd., and Yancheng Dyeing and Printing Co., Ltd., for their offer of some chemicals and for their generous funding. All financial support is gratefully acknowledged.

REFERENCES

1. Guillaume, C.; Ali, A.; Frédéric, B.; Bruno, A. *Prog. Polym. Sci.* **2011**, *36*, 1521.
2. Kreuer, K. D. *J. Membr. Sci.* **2001**, *185*, 29.
3. Ludvigsson, M.; Lindgren, J.; Tegenfeldt, J. *J. Electrochim. Acta* **2000**, *45*, 2267.
4. Kai, K.; Phil, H. K.; Young, C. N. *J. Appl. Polym. Sci.* **2006**, *99*, 1415.
5. Samms, S. R.; Wasmus, S.; Savinell, R. F. *J. Electrochem. Soc.* **1996**, *143*, 1225.
6. Liwei, Z.; So-Ryong, C.; Zachary, H.; Jin-Soo, P.; Mark, R. W. *Chem. Eng. J.* **2012**, *204*, 87.
7. Ghassemi, H.; McGrath, J. E. *Polymer* **2004**, *45*, 5847.
8. Dinh, X. L.; Dukjoon, K. *J. Membr. Sci.* **2013**, *430*, 37.
9. Papadimitriou, K. D.; Neophytides, S. G.; Kallitsis, J. K. *J. Membr. Sci.* **2013**, *433*, 1.
10. Kobayashi, T.; Rikukawa, M.; Sanui, K.; Ogata, N. *Solid State Ionics* **1998**, *106*, 219.
11. Liyuan, Z.; Gang, Z.; Chengji, Z.; Zhongguo, L.; Hao, J.; Shuai, X.; Mingyu, L.; Dan, X.; Hui, N. *Int. J. Hydrogen Energy* **2013**, *38*, 12363.
12. Dimitrova, G. P.; Baradie, B.; Foscallo, D.; Poinsignon, C.; Sanchez, J. Y. *J. Membr. Sci.* **2001**, *185*, 59.
13. Miyatek, K.; Chikashige, Y.; Higuchi, E.; Watanabe, M. *J. Am. Chem. Soc.* **2007**, *129*, 3879.
14. Higashihara, T.; Matsumoto, K.; Ueda, M. *Polymer* **2009**, *50*, 5341.
15. Li, G.; Xie, J.; Cai, H. F.; Qiao, J. L. *Int. J. Hydrogen Energy* **2014**, *39*, 2639.
16. Gao, Y.; Robertson, G. P.; Guiver, M. D.; Mikhailenko, S. D.; Li, X.; Kaliaguine, S. *Macromolecules* **2005**, *38*, 3237.
17. Sakaguchi, Y.; Kitamura, K.; Nagahara, S.; Takase, S. *Polym. Prepr. Am. Chem. Soc.* **2004**, *45*, 56.
18. Matsumura, S.; Hlil, A. R.; Lepiller, C.; Gaudet, J.; Guay, D.; Shi, Z.; Holdcroft, S.; Hay, A. S. *Macromolecules* **2008**, *41*, 281.
19. Miyatek, K.; Yasuda, T.; Hirai, M.; Nanasawa, M.; Watanabe, M. *J. Polym. Sci. Part A: Polym. Chem.* **2007**, *45*, 157.
20. Jung, E. Y.; Chae, B.; Kwon, S. J.; Kim, H. C.; Lee, S. W. *Solid State Ionics* **2012**, *216*, 95.
21. Xu, T. W.; Wu, D.; Wu, L. *Prog. Polym. Sci.* **2008**, *33*, 894.
22. Li, Q. F.; Jensen, J. O.; Savinell, R. F.; Bjerrum, N. *J. Prog. Polym. Sci.* **2009**, *34*, 449.
23. Li, X. P.; Liu, C.; Zhang, S. H.; Yu, G. P.; Jian, X. G. *J. Membr. Sci.* **2012**, *423*, 128.
24. Lin, H. L.; Hu, C. R.; Lai, S. W.; Yu, T. L. *J. Membr. Sci.* **2012**, *389*, 399.
25. Zhou, T. C.; Zhang, J.; Qiao, J. L.; Liu, L. L.; Jiang, G. P.; Zhang, J.; Liu, Y. Y. *J. Power Sources* **2013**, *227*, 291.
26. Zhou, T. C.; Zhang, J.; Fu, J.; Jiang, G. P.; Zhang, J.; Qiao, J. L. *Synth. Met.* **2013**, *167*, 43.
27. Fu, R. Q.; Hong, L.; Lee, J. Y. *Fuel Cells* **2008**, *8*, 52.
28. Lin, C. W.; Huang, Y. F.; Kannan, A. M. *J. Power Sources* **2007**, *164*, 449.
29. Xiong, Y.; Fang, J.; Zeng, Q. H.; Liu, Q. L. *J. Membr. Sci.* **2008**, *311*, 319.
30. Kim, D. S.; Park, H. B.; Rhim, J. W.; Lee, Y. M. *J. Membr. Sci.* **2004**, *240*, 37.
31. SeeponkaiI, N.; Wootthikanokkhan, J. *J. Appl. Polym. Sci.* **2007**, *105*, 838.
32. Qiao, J. L.; Tatsuhiro, O.; Hiroyuki, O. *Solid State Ionics* **2009**, *180*, 1318.
33. Thanganathan, U.; Nogami, M. *Int. J. Hydrogen Energy* **2015**, *40*, 1935.
34. Gomes, A. S.; Filho, J. C. D. *Int. J. Hydrogen Energy* **2012**, *37*, 6246.
35. Walsby, N.; Paronen, M.; Juhanoja, J.; Sundholm, F. *J. Appl. Polym. Sci.* **2001**, *81*, 1572.

36. Nasef, M. M.; Saidi, H.; Nor, H. M. *J. Appl. Polym. Sci.* **2000**, *77*, 1877.
37. Walsby, N.; Sundholm, F.; Kallio, T.; Sundholm, G. *J. Polym. Sci. Part A: Polym. Chem.* **2001**, *39*, 3008.
38. Brack, H. P.; Büchi, F. N.; Huslage, J.; Rota, M.; Scherer, G. G. In Membrane Formation and Modification; Pinnau, I., Freeman, B. D., Eds.; ACS Symposium Series 744; Oxford University Press: New York, **2000**; p 174.
39. Song, F. F.; Fu, Y. S.; Gao, Y.; Li, J. D.; Qiao, J. L.; Zhou, X. D.; Liu, Y. Y. *Electrochim. Acta* **2015**, *177*, 137.
40. Qiao, J. L.; Zhang, J.; Zhang, J. J. *J. Power Sources (Short Commun.)* **2013**, *237*, 1.
41. Zhang, J.; Qiao, J. L.; Liu, L. L.; Jiang, G. P.; Liu, Y. Y. *J. Power Sources* **2013**, *240*, 359.
42. Qiao, J. L.; Fu, J.; Lin, R.; Ma, J. X.; Liu, J. S. *Polymer* **2010**, *51*, 4850.
43. Kaiser, V.; Stropnik, C.; Musil, V.; Brumen, M. *Eur. Polym. J* **2007**, *43*, 2515.
44. Yi, Z.; Zhu, L.; Xu, Y.; Zhao, Y.; Ma, X.; Zhu, B. *J. Membr. Sci.* **2010**, *365*, 25.
45. Chen, N. P.; Hong, L. *Solid State Ionics* **2002**, *146*, 377.
46. Qiao, J. L.; Hamaya, T.; Okada, T. *Polymer* **2005**, *46*, 10809.
47. Kim, D. S.; Park, I. C.; Cho, H. I.; Kim, D. H.; Moon, G. Y.; Lee, H. K.; Rhim, J. W. *J. Ind. Eng. Chem.* **2009**, *15*, 265.
48. Holland, B. J.; Hay, J. N. *Polymer* **2002**, *43*, 2207.
49. Wang, J.; Yuan, H. L.; Huo, Y. L. *J. Beijing Univ. Chem. Technol.* **2005**, *32*(2), 68.
50. Sung, K. L.; Byong, C. B.; Ji, S. I.; Se, J. I.; Young, S. L. *J. Ind. Eng. Chem.* **2010**, *16*, 891.
51. Liu, W.; Chen, L.; Wang, Y. Z. *Polym. Degrad. Stab.* **2012**, *97*, 2487.
52. Kreuer, K. D.; Paddison, S. J.; Spohr, E.; Schuster, M. T. *Chem. Rev.* **2004**, *104*, 4637.
53. Qiao, J. L.; Hamaya, T.; Okada, T. *J. Mater. Chem.* **2005**, *15*, 4414.
54. Einsla, B. R.; Kim, Y. S.; Hickner, M. A.; Hong, Y. T.; Hill, M. L.; Pivovar, B. S.; McGrath, J. E. *J. Membr. Sci.* **2005**, *255*, 141.
55. Li, L.; Zhang, J.; Wang, Y. *J. Membr. Sci.* **2003**, *226*, 159.
56. Chikashige, Y.; Chikyu, Y.; Miyatake, K.; Watanabe, M. *Macromolecules* **2005**, *38*, 7121.
57. Yasuda, T.; Miyatake, K.; Hirai, M.; Nanasawa, M.; Watanabe, M. *J. Polym. Sci. Part A: Polym. Chem* **2005**, *43*, 4439.
58. Yamaguchi, T.; Kuroki, H.; Miyata, F. *Electrochem. Commun* **2005**, *7*, 730.
59. Santamaria, M.; Pecoraro, C. M.; Quarto, F. D; Bocchetta, P. *J. Power Sources* **2015**, *276*, 189.